Werk

Jahr: 1987
Kollektion: fid.geo
Signatur: 8 Z NAT 2148:61
Digitalisiert: Niedersächsische Staats- und Universitätsbibliothek Göttingen
Werk Id: PPN1015067948_0061
PURL: http://resolver.sub.uni-goettingen.de/purl?PPN1015067948_0061

LOG Id: LOG_0022
LOG Titel: Aqueous maghemitization of titanomagnetite
LOG Typ: article

Übergeordnetes Werk

Werk Id: PPN1015067948
PURL: http://resolver.sub.uni-goettingen.de/purl?PPN1015067948
OPAC: http://opac.sub.uni-goettingen.de/DB=1/PPN?PPN=1015067948

Aqueous maghemitization of titanomagnetite

K. Brown* and W. O'Reilly

Department of Geophysics and Planetary Physics, School of Physics, University of Newcastle upon Tyne, Newcastle upon Tyne NE1 7RU, U.K.

Abstract. Finely ground, sub-micron synthetic sintered titanomagnetite ($Fe_{2.4}Ti_{0.6}O_4$, TM60) and a chemical precipitated magnetite (the pigment Mapico Black – nominally Fe_3O_4) have been heated at 100° C in de-ionized water and sea water for times up to 60 days. Chemical analysis of the solid phases shows that considerable oxidation has taken place (about halfway to complete oxidation) and analysis of the liquid phase shows that iron has been removed from the solid. Magnetic studies of the oxidized material reveal at least two magnetic phases (i.e. spinel oxides) which cannot, however, be distinguished in the X-ray powder pictures of such fine material. The data is interpreted in terms of a grinding-induced strained surface layer which persists during the oxidation and determines the relative concentrations of the two magnetic phases (designated "skin" and "core"). In the present experiments, skin:core = 1:10. While the grain as a whole is oxidizing, the skin reduces and the core oxidizes. The magnetic properties of the solid phases are also consistent with iron removed by aqueous oxidation being incorporated into a third iron-rich spinel phase.

Introduction

Maghemitization

The primary magnetic mineral in the upper layers of the newly constructed Earth's crust at the spreading centres can be modelled by the composition $Fe_{2.4}Ti_{0.6}O_4$ (TM60). During construction of the crust or during sea-floor spreading, the TM60 may be altered by a number of processes – deuteric oxidation, subsolvus exsolution, maghemitization and inversion. (e.g. O'Reilly, 1984). In the course of maghemitization the TM60 becomes oxidized but maintains the spinel crystal structure. This implies an increasing degree of non-stoichiometry achieved by the introduction of cation vacancies, together with an increasing Fe^{3+}/Fe^{2+} ratio. The small size of vacancies and Fe^{3+} results in a shrinking of the spinel lattice. When the extent of maghemitization is non-uniform throughout a crystallite, the strain of lattice mismatch may be relieved by cracking within the particle; maghemitization may bring about microstructural, in addition to compositional, change. Separate particles, e.g., of haematite (αFe_2O_3), may be produced in connection with

or as a consequence of maghemitization. The cation-deficient spinel structure is metastable and may collapse to a more stable configuration (inversion) depending on the time-temperature-pressure regime.

Evidence from nature

The existence of titanomaghemite in basalts has long been established (e.g. Basta, 1959; Akimoto and Katsura, 1959). The recovery of basement material from the ocean floors and the discovery of widespread maghemitization (e.g. Marshall and Cox, 1972; Ryall and Hall, 1975; Petersen et al., 1979) led to an accelerated interest in the phenomenon. The observations of naturally occurring titanomaghemite suggest that oxidation might take place largely by the removal of iron from the crystallites rather than the addition of oxygen (Prévot et al., 1968; Marshall and Cox, 1972; Furuta et al., 1985).

Some indication of the physical conditions needed to bring about inversion of titanomaghemites may be found from naturally occurring material. Titanomaghemites have been found to sub-bottom depths of the order of 500 m, in basalts recovered from Hole 504B of the Deep Sea Drilling Project (O'Donovan and O'Reilly, 1983) but not below depths of about 800 m in the same hole (Facey et al., 1985).

Laboratory experiments

Geological time allows maghemitization of large grains (in the optical range), although often heterogeneously. In laboratory times, the upper limit to the temperature stability field of titanomaghemites ($\sim 350°$ C) has restricted successful simulations of the process to sub-optical particles. Oxidation has generally been carried out by heating in air and the progress of the reaction often monitored by gravimetry (e.g. Readman and O'Reilly, 1970). Differential thermogravimetric analysis (DTG) reveals two peaks in reaction rate which have been ascribed to the differential oxidation of Fe^{2+} on the two sublattices of the spinel structure (next section). The maghemitization of Mg-substituted (O'Donovan and O'Reilly, 1978) and Al-substituted TM60 (Özdemir and O'Reilly, 1981) has also been studied. Keefer and Shive (1981) and Nishitani and Kono (1983) have also synthesized and measured the Curie-point temperatures (T_c) and lattice parameters of titanomaghemites. Curie-point temperature rises, and lattice constant falls, as oxidation proceeds. The room-temperature spontaneous magnetization generally falls although it may rise again, e.g., in highly maghemitized

* *Present address:* RAE, Farnborough, Hampshire

substituted TM60. The characteristics of the magnetization process in fine-grain titanomaghemite have also been reported, including thermoremanence (TRM) (Özdemir and O'Reilly, 1983).

An exploration of oxidation of TM60 and magnetite in an aqueous environment has been described by Brown (1981) (the present paper contains the first full account of this work). Water had traditionally been ascribed an important role in the maghemitization of magnetite, being either associated with precipitated starting material, included in the oxidizing atmosphere, or introduced by pulverizing the starting material in water (Elder, 1965; Sakamoto et al., 1968). A small particle size and enhanced diffusion rates due to internal imperfections also seem to be essential to successful maghemitization. The role of water has not been entirely resolved, as gravimetry reveals that even acetone-ground finely divided starting materials contain adsorbed volatiles (presumably water) possibly gained from the atmosphere. Aharoni et al. (1962) suggested that maghemite is in fact a solid solution between model non-stoichiometric maghemite $Fe_{8/3}^{3+}O_4^{2-}$ and stoichiometric hydrogen ferrite $H_{1/2}^{+}Fe_{5/2}^{3+}O_4^{2-}$. In the Worm and Banerjee (1983) study of aqueous oxidation of titanomagnetite, hydrogen is also suggested to play a role, although principally as a sink for electrons. The progressive laboratory oxidation of basalt heated in sea water is suggested by the rise in Curie-point temperature of basalts with time of heating (Ryall and Hall, 1979).
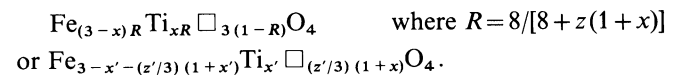
The inversion of natural or synthetic titanomagnetite during laboratory thermomagnetic experiments has been widely observed and is a useful qualitative and potentially quantitative indicator of maghemitization (O'Reilly, 1983).

Modelling the maghemitization process

Models involve the diffusion of ions within the body of the crystal together with the transfer of electrons between species (oxidation and reduction) at the surface of the crystal. Fe^{2+} situated on the tetrahedral sublattice and bonded covalently are believed to be less freely available for oxidation than ionically bonded octahedrally sited ions. The evidence for this comes from Mössbauer-effect spectra of simple spinels (Armstrong et al., 1966), diffusion experiments on Fe^{2+}-containing spinels (Freer and O'Reilly, 1980) and DTG analyses of the oxidation of titanomagnetite (Özdemir and O'Reilly, 1981). In addition to a factor describing the relative availability for oxidation of the Fe^{2+} on tetrahedral and octahedral sites, a further parameter of the models assigns the distribution of the produced vacancies to the sublattices. The first approximation – vacancies on octahedral sites only – is often adopted (O'Reilly, 1983), although the presence of a fraction on tetrahedral sites is probably needed to match models to experimental saturation magnetization data (Readman and O'Reilly, 1972). At the surface, the addition-of-oxygen (AO) mechanism results in an extension of the crystal structure; the number of cations remains constant and lattice vacancies are produced. The removal of metals (RM) implies a constant number of unit cells in the particle, lattice vacancies following from the removal of metals. O'Reilly (1983) envisages Fe^0 atoms, momentarily produced at the surface during electron hopping between Fe cations, being leached away through the attraction of a suitable medium. This suggests that oxidation by removal of Ti would require the simultaneous presence of Ti^{3+} and

Ti^{4+} and an electron hopping process. Worm and Banerjee (1983) propose that the removal of electrons from the Fe^{2+} ions in the crystal (oxidation) is not effected by escaping Fe^0, but that they are removed and collected by H^+ ions in aqueous solution whilst Fe^{2+} ions simultaneously exit from the crystal.

The effect of oxidation by the AO or RM on composition is shown in the ternary diagram of Fig. 3. Positions within the titanomaghemite quadrilateral may be assigned composition coordinates either (x, z) or (x', z'), the latter being most appropriate when considering oxidation by removal of iron. Lines of constant x' and z' are not parallel however, nor is z' linear in the diagram. A titanomaghemite at a given point in the quadrilateral, which may have been arrived at by a horizontal AO track or an inclined RM track, can be expressed (O'Reilly, 1983) in either set of coordinates as

$$Fe_{(3-x)R}Ti_{xR}\square_{3(1-R)}O_4 \qquad \text{where } R = 8/[8+z(1+x)]$$

or $Fe_{3-x'-(z'/3)(1+x')}Ti_{x'}\square_{(z'/3)(1+x)}O_4$.

The cation distribution in the titanomaghemite depends on the parameters describing both the internal and surface processes. O'Reilly's (1983) model cation distributions suggest that while the difference in saturation magnetization (M_s) of a given composition arrived at by the two mechanisms may be significantly different, the Curie-point temperature –being strongly sensitive to bulk composition but only weakly so to cation distribution – will be negligibly different.

The present study

The properties of air-synthesized titanomaghemites (principally T_c) have been successfully used to produce large-scale models of the geochemistry of the magnetic minerals of the submarine crust (Petersen et al., 1979). The general validity of such models is probably not seriously weakened by the use of air-oxidized synthetic analogues, as T_c is probably not significantly different (O'Reilly, 1983). The presence of other cation species (Al, Mg, Mn etc.) is a more serious difficulty, at least for detailed modelling. The use of air-oxidized materials as a data source for geophysical models of the submarine crust is more problematic. Saturation magnetization (and, by implication, the magnetization process parameters) may be quite different in a given composition produced by either the AO or RM mechanisms.

The present study describes an exploration of the oxidation of titanomagnetite in the laboratory when the AO mechanism is suppressed and the RM mechanism encouraged. The intention is not to make an accurate simulation of the complex system with many degrees of freedom such as operates on and under the sea floor. The principal questions to be addressed are: (i) can oxidation take place by removal of Fe; (ii) will Ti also be removed; (iii) are the intrinsic magnetic properties (T_c, M_s) of RM-produced materials significantly different from AO-produced titanomaghemite?

Experimental

Synthesis and characterization of starting material

Synthetic TM60 was prepared by twice-firing pressed pellets of Fe, Fe_2O_3 and TiO_2 mixed in stoichiometric proportions

in a $CO_2 - CO$ mixture appropriate to TM60 at the firing temperature (1350° C). The details of the procedure may be found elsewhere (e.g. Özdemir and O'Reilly, 1981). X-ray powder pictures revealed only the presence of a well-crystallized spinel phase with extrapolated cell edge 8.478 ± 0.002 Å using the method of Nelson and Riley (1945). Using the extrapolation method of Fig. 2, a Curie-point temperature of 176° C was derived from the temperature dependence of saturation magnetization of a piece of pellet. Using the Hauptman (1974) relationship $T_c = 149 + 712z$ (°C), the oxidation parameter of the starting material was determined as $z = 0.038 \pm 0.003$. The initial susceptibility (a magnetization process parameter) fell rapidly at 171° C, slightly below T_c.

The grain size of the near-stoichiometric TM60 was reduced to about 0.1 μm by ball milling for times between 6 and 12 h in a high-purity methanol slurry. This was to increase the specific surface area, and so promote oxidation, and to simulate the fine-particle material of quenched submarine basalts. The slurry was dried at room temperature. As is commonly found, the maghemitization process had already begun during grinding. The X-ray powder pictures now showed additional lines which could be indexed as a tetragonal superstructure with the exception of one line ($d = 2.187$) which could be ascribed to haematite. Calculating a (rough) cell edge from the superstructure lines alone may suggest that part of the grains is oxidized and has a lower cell edge than the stoichiometric core. This is confirmed by high-field thermomagnetic analysis of encapsulated material for which the Curie point was observed at 194° C (9 h milled) and 222° C (12 h milled) on the heating cycle. After heating to 600° C, the cooling curves gave lower T_c values and ratios of magnetization after the cycle (M_F) to the starting value (M_I) greater than unity (1.2–1.3).

The composition of the finely ground material was determined by wet chemical volumetric analysis. The material was dissolved in 5 N hydrochloric acid with various precautionary measures to prevent oxidation during dissolution. Fe^{2+} concentration was determined by titration against 0.05 N ceric sulphate solution using 1:10 phenanthroline-ferrous sulphate as indicator. The titrated volume of standard solution was corrected for the presence of the indicator. Total iron was determined as Fe^{2+} by reducing the Fe^{3+} by adding 10% stannous chloride solution drop by drop to the hot solution. Excess Sn^{2+} in the solution was oxidized by the addition of a saturated solution of mercuric chloride. 0.05 N potassium dichromate was titrated against the sample using 0.2% barium diphenylamine as indicator together with Spekker acid to produce an unambiguous end-point. The method was checked against the pre-ground near-stoichiometric TM60. The resulting composition coordinates for the fine-ground TM60 were: $x = 0.66 \pm 0.06$; $z = 0.13 \pm 0.06$. This confirms that some oxidation had taken place during grinding. Once the material has become oxidized, and later during the oxidation experiments (next section), the x value changes from the starting value of 0.6 if iron has been removed from the spinel phase(s). We simply retain the blanket term TM60 for all samples in the present study derived from our starting sintered $x = 0.6$ material.

Hysteresis loops were run at room temperature in a maximum field of 9×10^5 A/m, the TM60 being dispersed in calcium fluoride (oxide:salt about 4% by volume) and pressed into pellets. Saturation magnetization in infinite field (σ_s) was determined by extrapolation using the expression $\sigma = \sigma_s(1 - b/H^2)$. This yielded $\sigma_s = 24 \pm 1$ Am²/kg [and $b = (1.4 \pm 0.3) \times 10^{10}$ A²/m²], a good value for fine-particle TM60. Using the extrapolated saturation magnetization, the ratio of saturation remanence to saturation magnetization (M_{rs}/M_s) of 0.5 ± 0.03 seems to indicate non-interacting randomly oriented monodomain grains with uniaxial anisotropy. (This does not exclude, of course, the possibility of cubic anisotropy with M_{rs}/M_s reduced from the model value of 0.7 by the presence of superparamagnetic grains, or grains containing some domains, or interactions between grains; the obtained value of 0.5 would then be only a coincidence.) The coercive force of $(9.0 \pm 0.1) \times 10^4$ A/m and initial susceptibility 0.34 ± 0.02 are explicable in terms of an average internal stress of about 10^8 N/m² together with a magnetostriction coefficient λ_s of 2.1×10^{-4}.

A second starting composition was provided by a commercially produced pigment, "Mapico Black". This is manufactured by the Columbia Carbon Company (who kindly provided the sample). The material, which has grain size 0.2–0.8 μm and is prepared at low temperature, is typical of the kind of magnetite which readily oxidizes in air to produce magnetite-maghemite solid solution. It therefore provides a different type of starting material to the sintered TM60 and contains negligible titanium. X-ray powder pictures were consistent with a spinel structure having extrapolated cell edge 8.393 ± 0.001 Å. Faint haematite lines were also present. Chemical analysis showed that, like the fine-particle TM60, the Mapico Black was also partially maghemitized although to a greater extent. The composition coordinates returned by the analysis were : $x = 0.01 \pm 0.06$ and $z = 0.34 \pm 0.06$. High-field thermomagnetic analysis of an encapsulated sample gave a Curie-point temperature of $579° \pm 5°$ C and M_F/M_I near to unity. The saturation magnetization ($\sigma_s = 79 \pm 3$ Am²/kg) was low compared to the 92 Am²/kg expected for pure unoxidized magnetite. Otherwise the M_{rs}/M_s of 0.275 ± 0.005 and H_c of $(2.59 \pm 0.03) \times 10^4$ A/m are typical of fine-grain magnetite.

Oxidation in water

The experiments were carried out at 100° C to accelerate, into the laboratory time scale, the reaction which may take place in the order of 10^6 year during submarine weathering. In a standard run, 1 g of oxide was heated in 500 ml of de-ionized water or sea water in glass apparatus under atmospheric pressure for times between 1 and 60 days, the liquid volume maintained by a reflux condenser. The sea water was collected 20 km from the coast of NE England. At the end of a run, the liquid was decanted off and filtered. The solid phase was dried by blowing with cold air. The iron and titanium content of the liquid was determined immediately after the run by atomic absorption spectroscopy and the composition of the solid phase determined by wet chemical analysis. The results are presented in Table 1 in the form of total iron in the aqueous phase (from a starting 1-g solid phase) and the composition of the solid material expressed as z (salt in sea-water-heated solid material having been allowed for). If oxidation had taken place only by removal of iron *and* all the iron remained in solution, then the change in z which can be calculated from the concentration of the water-borne iron should be consistent with the change in z of the solid phase. However, the iron concentrations are about 10% of the values needed

Table 1. Chemical analysis of the aqueous and solid products after heating TM60 and Mapico Black in de-ionized water (DW) or sea water (SW) at 100° C for times up to 60 days

Heating time (days)	TM60				TMO (Mapico Black)			
	Iron in aqueous phase (μg)		Composition of solid (z)		Iron in aqueous phase (μg)		Composition of solid (z)	
	DW	SW	DW	SW	DW	SW	DW	SW
0	15	220	0.13	0.13	15	220	0.34	0.34
1	15	220	0.16	0.22	0	240	0.42	0.46
2	0	420	0.26	0.26	30	230	0.45	0.49
7.5	30	660	0.29	0.34	200	275	0.48	0.42
15	50	240	0.21	0.20	–	243	–	0.39
30	240	180	0.44	0.20	9	190	0.51	0.55
60	1300	3000	0.20	0.37	1300	200	0.42	0.36

to account for the change in composition of the solid phase. This means that if, at one extreme, oxidation has taken place only by removal of iron, the capacity of the liquid part of the system is not large enough to carry the removed iron and that about 90% of the removed iron has become part of the solid phase leaving about 10% in solution. At the other extreme, 90% of the oxidation has taken place by addition of oxygen to the solid phase and 10% by removal of iron which has gone into solution. Intermediate proportions of the two mechanisms operating in tandem are possible, but it is clear from the presence of iron in solution that removal of iron plays a significant role in the alteration process. No titanium was found in the aqueous phase.

Analysis of the reaction kinetics is not possible, as can be seen from the erratic relation between heating time and the extent of oxidation achieved in the separate runs. The scatter is not due to uncertainties in the analysed compositions. These correlate satisfactorily with the compositions as expressed in the Curie-point temperatures (Fig. 2), and the estimated uncertainties in the water-borne iron and the solid-phase z values are typically ± 20 μg and ± 0.05, respectively. The scatter results from inadequate control of the experimental conditions under which the solid/liquid reaction takes place. In some runs the boiling water "bumped" violently.

The general conclusions which can be reached are that (i) oxidation has taken place in the aqueous environment, (ii) iron is removed from the crystal and this process accounts for at least 10% of the oxidation achieved, (iii) titanium is not removed.

The X-ray powder pictures of the solid material remained essentially unchanged during aqueous oxidation with a trend of scattered spinel cell edges decreasing with increasing heating time.

Magnetic properties of the oxidized material

Thermomagnetic analysis. Specimens of the oxidized material were heated in evacuated capsules to 700° C in the magnetic balance in a field of about 3×10^5 A/m. As titanomaghemites are structurally metastable, the heating and cooling parts of the thermomagnetic cycle are different. In order to produce a set of comparable cooling ($M_s - T$) curves, the runs were standardized by holding the specimen
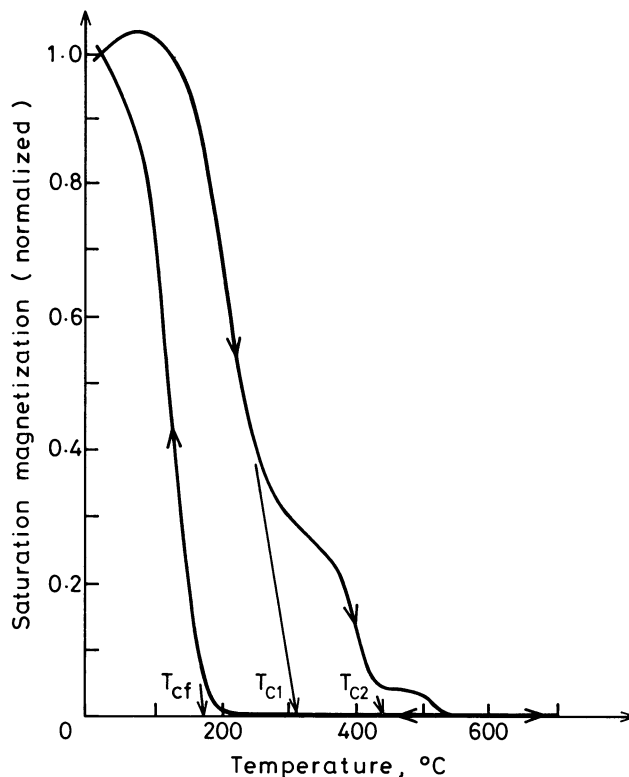

Fig. 1. Thermomagnetic curve of encapsulated TM60 previously heated in de-ionized water for 30 days. T_{c1} and T_{c2} are the Curie points observed on the heating run. This particular sample also shows a heating-run Curie point at 540° C. T_{cf} is the final Curie point on cooling after holding the specimen at 700° C

Table 2. Parameters of the thermomagnetic runs on encapsulated specimens of oxidized TM60. T_{c1} and T_{c2} are Curie-point temperatures observed during the heating run and T_{cf} that observed on the cooling run after holding the specimen at 700° C for 2 h

Heating time (days)	De-ionized water			Sea water		
	T_{c1}	T_{c2}	T_{cf}	T_{c1}	T_{c2}	T_{cf}
0	222		190	222		190
1	258	580	181	242	410	157
2	274	560	185	254	420	160
7.5	296	490	205	280	560	188
15	260	550	180	260	420	174
30	312	450,540	174	304	440	169
60	335	460,580	187	317	410	170

for 2 h at 700° C before cooling, with the purpose of allowing the process of inversion to go to completion.

The thermomagnetic curve of TM60 heated in de-ionized water for 30 days is shown in Fig. 1. In general, at least two Curie points were observed on the heating run (this more oxidized sample shows three – one at 540° C) and, after holding the temperature at 700° C for 2 h, a single low Curie point on the cooling run. The Curie-point temperature data for the oxidized TM60 suite are summarized in Table 2. For the Mapico Black suite, single Curie points were observed on both heating and cooling runs, all at between 570° and 585° C. The TM60 data are plotted in Fig. 2 now with z, the composition of the solid phase, as a variable rather than heating time as in Table 2. As degree
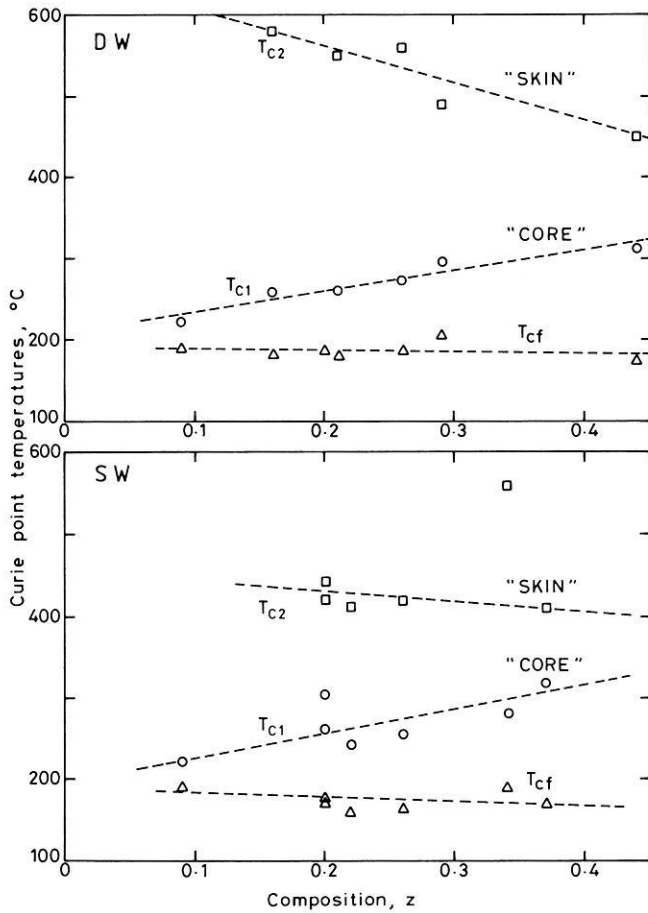
Fig. 2. Curie-point temperatures T_{c1}, T_{c2} and T_{cf} plotted against composition for the oxidized TM60. The *upper figure* shows the result for the de-ionized water runs (*DW*) and the *lower figure* the sea water runs (*SW*). The *dashed lines* are not models, but indicate perceived trends

of oxidation increases, a rise in T_{c1} and a fall in T_{c2} are indicated; T_{cf} remains constant. The data points for 60 days in de-ionized water have been omitted from the plot. The z value (0.20) of Table 1 seems anomalously low compared to the magnetically inferred z suggested by the T_{c1} and T_{c2} values. From the trends of Fig. 2 a z of about 0.4 would be indicated. The M_F/M_I values ranged between about 0.8 and 1.3 and showed no discernible trends with degree of alteration.

Hysteresis loop parameters and saturation magnetization. The data are listed in Table 3a and b. No significant changes in saturation magnetization (σ_s) or the ratio of saturation remanence to saturation magnetization (σ_{rs}/σ_s) is observed as alteration proceeds. The coercive force (H_c) data is more complex. This is because one batch of milled TM60 exhibited slightly waisted hysteresis loops (perhaps the grain size of this batch was small enough to contain near-superparamagnetic particles) and gave reduced coercive forces. In Table 3(a), coercive forces $< 10^5$ A/m correspond to the waisted loops and those $> 10^5$ A/m to the non-waisted loops. An additional, and unavoidable, complication in the magnetization process data is that the parameters depend on more than one variable, whereas the Curie-point temperatures depend on only one – the composition. σ_{rs}/σ_s and

H_c depend on composition and microstructure and the dependence is even more complex in an assemblage of (say) two compositions, each with its own microstructure. σ_s depends on composition and also on concentration in a system containing more than one phase.

Discussion

The course of alteration

The chemical analysis (Table 1) shows that appreciable oxidation of the TM60 (up to $z \sim 0.4$) has taken place in water in times up to 60 days at 100° C, and that the removal of iron from the solid has contributed to this process. In addition to the chemical analysis, the thermomagnetic data (Fig. 2) also provides evidence for the compositional changes proceeding during oxidation. The reaction rates compare favourably with air-oxidation studies. To produce a z of 0.425 in a similar TM60 starting material, Özdemir & O'Reilly (1981) record the following treatment: 1.5 h at 100° C, 20 h at 130° C, 12 h at 165° C. The much longer times of the present experiments ($\sim 10^2$–10^3 h) may be largely explicable in terms of the lower alteration temperature. Assuming the reaction rate is proportional to $\exp(-Q/kT)$, and taking $Q = 1$ eV, the reaction rate at 200° C is about 10^3 greater than that at 100° C. To obtain higher degrees of alteration in times of the order of tens of hours, air-oxidation treatment temperatures rise to about 300° C, where the same calculation suggests the reaction rate is about 10^5 times greater than at 100° C.

The thermomagnetic analysis shows that at least two phases are present in the oxidized material – one associated with T_{c1}, which rises with z from near the Curie point of the starting material; and another with T_{c2}, which appears early in the alteration procedure and subsequently falls as z increases. The two Curie points may converge at about $z = 0.6$ by extrapolation of the data of Fig. 2. The resolution of the two phases, which are both almost certainly spinels, is not allowed by the quality of the X-ray powder pictures of such finely divided material.

The composition of the alteration products

We propose the following scenario which is broadly consistent with the observations.

During grinding a strained surface layer is formed which is readily maghemitized; indeed, the extent of grinding-induced oxidation is largely accounted for by the oxidation of the strained layer. At the beginning of maghemitization at elevated temperature, the strained layer rapidly attains maximum oxidation state. We assign T_{c1} to the largely unaltered "core" and T_{c2} to the highly oxidized "skin". The persistence of T_{c1} and T_{c2} up to $z \sim 0.5$ implies that the core and skin remain as distinct regions of the grains up to this degree of oxidation; the changing values of T_{c1} and T_{c2} reflect the changing compositions of core and skin. During air-induced maghemitization of finely ground material at higher temperatures, the higher diffusion rates within the crystal presumably account for the absence of distinct phases. The thermomagnetic analysis of such air-oxidized materials shows only one Curie point, although it may be less well defined than in large-grain unoxidized samples.
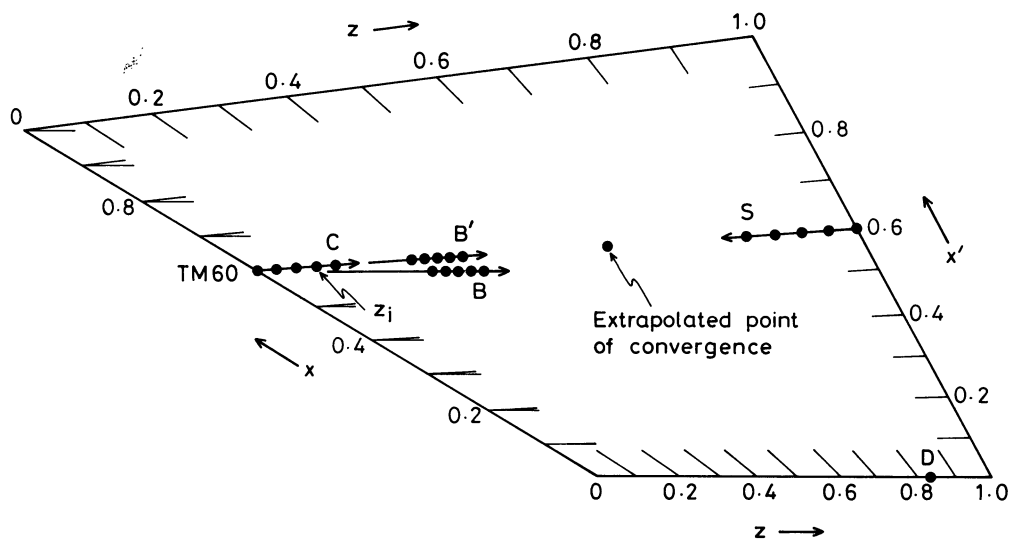
The chemical composition of "core" (C) and "skin" (S) are shown in Fig. 3. In the figure we have assumed

Table 3a. Saturation magnetization (σ_s) and the magnetization process parameters σ_{rs}/σ_s (ratio of saturation remanence to saturation magnetization) and H_c (coercive force) for oxidized TM60 (z is the degree of oxidation). Of the two sea-water $z=0.2$ specimens, the upper corresponds to the shorter oxidation time

De-ionized water				Sea water			
z	σ_s (Am^2/kg^{-1})	σ_{rs}/σ_s	H_c ($\times 10^4$ A/m^{-1})	z	σ_s (Am^2/kg^{-1})	σ_{rs}/σ_s	H_c ($\times 10^4$ A/m^{-1})
0.09	24	0.50	9.0	0.09	24	0.50	9.0
0.16	26	0.56	12.6	0.20	29	0.50	8.5
0.20	24	0.56	11.4	0.20	26	0.58	7.0
0.21	26	0.50	7.5	0.22	24	0.53	14.1
0.26	27	0.45	–	0.26	24	0.56	15.4
0.29	24	0.56	10.8	0.34	25	0.53	–
0.44	22	0.50	6.4	0.37	25	0.62	12.4

Tabelle 3b. Saturation magnetization (σ_s) and the magnetization process parameters σ_{rs}/σ_s (ratio of saturation remanence to saturation magnetization) and H_c (coercive force) for oxidized TMO (Mapico Black). Of the two $z=0.42$ de-ionized water-oxidized specimens, the upper corresponds to the shorter oxidation time

De-ionized water				Sea water			
z	σ_s (Am^2/kg^{-1})	σ_{rs}/σ_s	H_c ($\times 10^4$ A/m^{-1})	z	σ_s (Am^2/kg^{-1})	σ_{rs}/σ_s	H_c ($\times 10^4$ A/m^{-1})
0.33	80	0.28	2.59	0.33	80	0.28	2.59
0.42	78	0.26	1.1	0.36	82	0.15	1.14
0.42	79	0.15	1.16	0.39	88	0.16	1.19
0.45	80	0.17	0.97	0.42	82	0.17	1.28
0.48	77	0.16	1.26	0.46	–	0.18	1.5
0.51	77	0.18	1.38	0.49	81	0.18	1.56
				0.55	78	0.16	1.13

Fig. 3. Proposed evolution of the phases in the maghemitized TM60 showing the gradual oxidation of the "core" phase (C), the reduction of the "skin" phase (S), the approximate location of the removed and oxidized iron (D) and the migration of the bulk composition of the solids (B) and the maghemitized grains (B'). C, S and B' converge at about $z=0.6$ C having started at $z=0$, S at $z=1$ and B' at $z=0.1$

oxidation by removal of iron. If the iron is contained as Fe_2O_3 in the solid phase together with the maghemitized grains, then the presence of this material (D) can also be indicated on the figure. This could possibly be an $Fe_3O_4/\gamma-Fe_2O_3$ highly oxidized phase as suggested by the analysis of the saturation magnetization data (next section). The bulk composition of the solid phase lies at B and the bulk

composition of maghemitized grains at B'. As oxidation proceeds, the location of the core moves to the right (T_{c1} rises) whereas that of the skin moves to the left (T_{c2} falls). The bulk compositions B and B' move to the right. The quantity of D increases. When z reaches about 0.6, the compositions at C and S will have converged on B'. The chemical analysis of Table 1 yields the composition of B.

For simplicity we shall ignore the small difference in the z values of B and B' so that if z_c is the composition of the core, z_s the composition of the skin and the skin accounts for an average fraction f of the grains, then (the bulk) $z = (1-f) z_c + f z_s$. As T_{c1} and T_{c2} can be taken to vary linearly with the bulk composition (Fig. 2), we also suppose their associated compositions can similarly be taken to change in a linear manner. Assigning an initial value of $z = z_i$ which corresponds to the initial rapid oxidation of the strained layer, and taking $z_c = 0$ and $z_s = 1$ at z_i, then $z_c = a(z - z_i)$ and $z_s = 1 - b(z - z_i)$, where a and b are constants. Substituting for z_c and z_s in the expression for the bulk composition yields $f = \{z - a(z - z_i)\}/\{l - (a + b)(z - z_i)\}$. Determination of numerical values for a, b and z_i will reveal the variation in concentration of the core and skin as maghemitization progresses.

A value $z_i = 0.1$ is indicated from Table 1 (and is typical of the post-ground state of titanomagnetite of previously published studies). This implies that the strained layer occupies a fraction 0.1 of the grains. Taking $z_c = z_s = z$ at $z = 0.6$ (Fig. 2), then $a = 1.2$ and $b = 0.8$. These values give $f = 0.1$, independent of z. The strained surface layer therefore appears to be a dominant factor in these low-temperature experiments, persisting throughout the oxidation process and dictating what the coexisting compositions and concentrations of the consequent two phases will be for a given bulk composition. When the skin contains a higher concentration of Fe^{3+} and $\square$ and a lower concentration of Fe^{2+} than the core, the resultant diffusion across the boundary can be represented by $(2/3\ Fe^{3+} + 1/3\ \square)$ entering the core for each Fe^{2+} leaving. There is a net loss of iron from the core, and the increased Fe^{3+} concentration results in the rise in T_{c1}. The increased Fe^{2+} concentration in the skin leads to the fall in T_{c2}. The core oxidizes and the skin reduces, while the grain as a whole oxidizes. The rate of oxidation of the whole grain will be controlled by the concentration of Fe^{2+} near the surface in the skin, so the whole grain cannot oxidize faster than the core (the source of Fe^{2+}).

The magnetic properties of the oxidized material

Having arrived at a model for the composition and concentration of coexisting skin and core, this model can, in principle, be tested against the measured saturation magnetization values. The room-temperature values of the saturation magnetization of single-phase titanomaghemites ($x = 0.6$) prepared by air oxidation can be represented by $\sigma_s(z) = 23(1 - 0.63z)$ Am²/kg (Özdemir and O'Reilly, 1983). For the present two-phase material $\sigma_s(z) = f\sigma_s(z_s) + (1 - f)\sigma_s(z_c)$. Substitution of numerical values for f, z_i, a and b gives a $\sigma_s(z)$ for the combined core and skin numerically the same as the single-phase material. Thus, $\sigma_s(z)$ should fall by about 30% when z reaches about 0.5.

The weighed specimen used to find the σ_s of Table 3a also includes the non-titanomaghemite phases. Taking 1 kg mol of $Fe_{3-x}Ti_xO_4$ to release $(z'/3)(1+x)$ Fe which in turn oxidizes to Fe_2O_3 and which is included with the weighed sample of solid phase, we find that 1 kg of solid derived by oxidation of TM60 contains $(1 - 0.13z')/(1 + 0.06z')$ kg of maghemitized TM60 and $0.19z'/(1 + 0.06z')$ kg of Fe_2O_3. Thus, for $z' \sim 0.5$ the measured σ_s for the mixed phases would be reduced by a factor of about 0.9 of the maghemitized TM60 alone (assuming negligible magnetiza-

tion of the Fe_2O_3), i.e. to about 55% of the starting TM60. This is clearly not borne out by the data of Table 3a.

A simple explanation of the disagreement is that the test is invalid because the cation distributions in water-oxidized TM60 are different to those in air-oxidized TM60. This is certainly the case in the model 0 K spontaneous magnetizations calculated by O'Reilly (1983). However, no room-temperature experimental σ_s values exist for single-phase water-oxidized material. A further means of resolving the problem and preserving the model for the two-phase grains is to suppose that the Fe_2O_3 is a magnetic material precipitated from the solution (like the Mapico Black). Perhaps this is detectable in the most highly oxidized samples (Fig. 1). Assigning a saturation magnetization of 80 Am²/kg to this phase, we arrive at $\sigma_s(z) = (23 - 2z + 1.89z^2)/(1 + 0.06z)$ Am²/kg for the mixed phases. Thus, for $z = 0.5$ the moment will have fallen from 23 to 22 Am²/kg – less than the scatter in the data.

The σ_{rs}/σ_s values suggest monodomain behaviour throughout for the TM60-derived suite. When several phases are present, the resultant coercive force depends on the relative concentrations of the phases in addition to the composition and grain size of the individual phases.

The Mapico Black, not necessarily having the strained layer of the ground TM60, may be more uniformly altered. The conversion of the removed iron to magnetic oxide phase would also be consistent with the negligible change in σ_s. The fall in magnetic hardness of Mapico Black following heat treatment is a commonly observed, but as yet unexplained, phenomenon (Dunlop, personal communication).

Thermomagnetic behaviour

The characteristic thermomagnetic signatures of inversion of titanomaghemite, either synthetic or in submarine basalts, are absent from the present data. There is no rise in magnetization above about 350° C during the heating run, with a fall towards about 600° C followed by a greatly enhanced magnetization observed in the cooling run. The different behaviour observed in the present investigation may be due to the samples being different to air-oxidized material, or due to the different procedure adopted in the present runs (a 2-h "soak" at 700° C). The lower non-stoichiometry of the core may discourage inversion; the stability of the core may be transferred to the more non-stoichiometric skin. Inversion may take place at higher temperatures than expected. The Curie point on the cooling run (T_{cf}) seems independent of the degree of oxidation and approximates closely to the starting TM60. It is tempting to suggest that the material has re-equilibrated to TM60 plus possibly non-magnetic phases after 2 h at 700° C in the evacuated capsule. Further experiments are needed.

Conclusions

Results

i) Titanomagnetite readily oxidizes in water, the reaction rates being comparable to air-oxidation experiments on similar materials.

ii) Oxidation proceeds, at least in part, by the removal of iron; there is no evidence for titanium removal.

iii) The oxidation product contains more than one magnetic phase.

Jiff

Interpretation

i) During pre-alteration grinding a strained surface layer is formed, constituting about 10% by volume of the grains. This layer persists during oxidation at low enough temperatures and results in the formation of two zones of different degree of oxidation – an initially highly oxidized "skin" and a near-stoichiometric "core".

ii) During oxidation the relative volumes of skin and core remain constant, but the compositions change as the whole grain gradually oxidizes; the core oxidizes and the skin reduces.

iii) Iron removed during oxidation is in turn oxidized by addition of oxygen and accumulates as a magnetic spinel phase with the maghemitized material. Thus, the saturation magnetization of the solid phases does not change significantly during oxidation and a third (high) Curie point becomes detectable in the more highly oxidized samples.

References

Aharoni, A., Frei, E.H., Schieber, M.: Some properties of γFe_2O_3 obtained by hydrogen reduction of αFe_2O_3. J. Phys. Chem. Solids **23**, 545–554, 1962

Akimoto, S., Katsura, T.: Magnetochemical study of the generalized titanomagnetite in volcanic rocks. J. Geomag. Geoelectr. **10**, 69–90, 1959

Armstrong, R.J., Morrish, A.H., Sawatzky, G.A.: Mössbauer study of ferric ions in the tetrahedral and octahedral sites of a spinel. Phys. Lett. **23**, 414–416, 1966

Basta, E.Z.: Some mineralogical relationships in the system $Fe_2O_3 - Fe_3O_4$ and the composition of titanomaghemite. Econ. Geol. **54**, 698–719, 1959

Brown, K.: Laboratory simulation of submarine maghemitization. Geophys. J.R. Astron. Soc. **65**, 273 (Abstract), 1981

Elder, T.: Particle size effect in oxidation of natural magnetite. J. Appl. Phys. **36**, 1012–1013, 1965

Facey, D., Housden, J., O'Reilly, W.: A magneto-petrological study of rocks from the Leg 83 section, Hole 504B of the Deep Sea Drilling Project. Initial Reports DSDP **83**, 339–346, 1985

Freer, R., O'Reilly, W.: The diffusion of Fe^{2+} ions in spinels with relevance to the process of maghemitization. Mineral. Mag. **43**, 889–899, 1980

Furuta, T., Otsuki, M., Akimoto, T.: Quantitative electron probe micro-analysis of oxygen in titanomagnetites with implications for oxidation processes. J. Geophys. Res. **90**, 3145–3150, 1985

Hauptman, Z.: High temperature oxidation, range of non-stoichi-

ometry and Curie point variation of cation deficient titanomagnetite $Fe_{2.4}Ti_{0.6}O_{4+y}$. Geophys. J.R. Astron. Soc. **38**, 29–47, 1974

Keefer, C.M., Shive, P.N.: Curie temperature and lattice constant reference contours for synthetic titanomaghemites. J. Geophys. Res. **86**, 987–998, 1981

Marshall, M., Cox, A.: Magnetic changes in pillow basalt due to sea-water weathering. J. Geophys. Res **77**, 6459–6469, 1972

Nelson, J.B., Riley, D.P.: An experimental investigation of extrapolation methods in the derivation of accurate unit cell dimensions of crystals. Proc. Phys. Soc. **57**, 160–177, 1945

Nishitani, T., Kono, M.: Curie temperature and lattice constant of oxidized titanomagnetite. Geophys. J.R. Astron. Soc. **74**, 585–600, 1983

O'Donovan, J.B., O'Reilly, W.: Cation distribution in synthetic titanomagnetites. Phys. Earth Planet. Inter. **16**, 200–208, 1978

O'Donovan, J.B., O'Reilly, W.: Magnetic properties of basalts from Hole 504B, DSDP Leg 69. Initial Reports DSDP **69**, 721–726, 1983

O'Reilly, W.: The identification of titanomaghemites: model mechanisms for the maghemitization and inversion processes and their magnetic consequences. Phys. Earth Planet. Inter. **31**, 65–76, 1983

O'Reilly, W.: Rock and mineral magnetism, 220 pp. Glasgow: Blackie; New York Chapman and Hall, 1984

Özdemir, Ö., O'Reilly, W.: Laboratory synthesis of aluminium substituted titanomaghemites and their characteristic properties. J. Geophys. **49**, 93–100, 1981

Özdemir, Ö., O'Reilly, W.: An experimental study of thermoremanent magnetization acquired by synthetic monodomain titanomaghemites. J. Geomag. Geoelectr. **34**, 467–478, 1983

Petersen, N., Eisenach, P., Bleil, U.: Low temperature alteration of magnetic minerals in ocean floor basalts. In: Deep sea drilling results in the Atlantic Ocean: ocean crust, Talwani et al., eds.: pp 169–209. Chelsea MI: Lithocrafters 1979

Prévot, M., Rémond, G., Caye, R.: Etude de la transformation d'une titanomagnetite en titanomaghémite dans une roche volcanique. Bull. Soc. Fr. Minéral. Crystallogr. **91**, 65–74, 1968

Readman, P.W., O'Reilly, W.: The synthesis and inversion of nonstoichiometric titanomagnetites. Phys. Earth Planet. Inter. **4**, 121–128, 1970

Readman, P.W., O'Reilly, W.: Magnetic properties of oxidized (cation-deficient) titanomagnetites (Fe, Ti, $\Box$)$_3$O$_4$. J. Geomag. Geoelectr. **24**, 69–90, 1972

Ryall, P.J.C., Hall, J.M.: Radial variation of magnetic properties in submarine pillow basalts. Can. J. Earth Sci. **12**, 1959–1969, 1975

Ryall, P.J.C., Hall, J.M.: Laboratory alteration of titanomagnetites in submarine pillow lavas. Can. J. Earth Sci. **16**, 496–504, 1979

Sakamoto, N., Ince, P., O'Reilly, W.: The effect of wet-grinding on the oxidation of titanomagnetites. Geophys. J.R. Astron. Soc. **15**, 509–515, 1968

Worm, H.-U., Banerjee, S.K.: Aqueous low-temperature oxidation of titanomagnetite. Geophys. Res. Lett. **11**, 169–172, 1983